

The Floating Kuroshio Turbine Blades Geometry Design with Consideration of the Structural Strength

Sin-An Lai¹, Ching-Yeh Hsin^{2*}, Chi-Fang Lee³, Tsung-Yueh Lin⁴, Jiahn-Horng Chen⁵

1) Student, Dept. of Systems Engineering and Naval Architecture, National Taiwan Ocean University, 2, Pei-Ning Rd., Keelung, Taiwan 20224

e-mail: sinanlai.sal@gmail.com

2) Professor, Dept. of Systems Engineering and Naval Architecture, National Taiwan Ocean University, 2, Pei-Ning Rd., Keelung, Taiwan 20224

e-mail: cy_hsin@hotmail.com

3) Engineer, CR Classification Society, 8th Fl., No.103, Sec. 3, Nanking E. Rd., Taipei, Taiwan 10491

4) Engineer, CR Classification Society, 8th Fl., No.103, Sec. 3, Nanking E. Rd., Taipei, Taiwan 10491

5) Professor, Dept. of Systems Engineering and Naval Architecture, National Taiwan Ocean University, 2, Pei-Ning Rd., Keelung, Taiwan 20224

Abstract

In this paper, two design procedures of the Floating Kuroshio Turbine blade geometries are presented. The first one is similar to the propeller design method, the Lagrange multiplier method with a lifting line method is used for the design of the loading distribution, and the lifting surface method is then adopted for the blade geometry design. The second design procedure uses Genetic Algorithm method and boundary element method (BEM) to improve the design from the first procedure. Hydrodynamic performances of the marine current turbine are then computed and analyzed by the potential flow boundary element method and the viscous flow RANS method. The BEM used here is a self-developed, perturbation potential based boundary element method, and a wake alignment numerical scheme is established for the current turbine. The viscous flow computations are carried out by the commercial CFD software STAR-CCM+. The design of a 20kw floating type Kuroshio turbine is demonstrated in the paper, and the design results show the geometries designed by the presented procedures can not only satisfy the hydrodynamic design goal, but also predict the delivered power very close to the experimental data. Finally, the structural strength of the turbine blade is computed by FEM, and the results are evaluated to see if the design complies the Rule requirements.

Keyword: Kuroshio, horizontal axis current turbine, blade design, boundary element method, RANS, FEM

1. INTRODUCTION

Two most common devices used for extracting the ocean current energy are the horizontal axis current turbine and the vertical axis current turbine. Most people use the wind turbine blade design methods for the horizontal axis current turbine design; however, the current turbines operate in the water, and their physical behaviours are more like marine propellers. In this paper, two turbine blade design procedures are presented, and the design case is demonstrated. One design procedure is similar to the propeller designs, and lifting line method [1-4], lifting surface design method [5-7], and boundary element method [8] are used. The other design procedure is to use Genetic Algorithm [9] to find a geometry which can provide the maximum torque and the minimum thrust. After completing the designs, both the boundary element method and the viscous flow RANS method [10-11] are applied to the analysis of the performances of the current turbines for the final check of the designs. After the blade geometry is designed, the finite element method is then used to analyze the blade structural strength, and the results are evaluated to see if the design complies the Rule requirements.

2. HYDRODYNAMIC ANALYSIS METHOD

Two computational methods are used for the current blade performance analysis, and they are the potential flow boundary element method (BEM) and viscous flow RANS method. The commercial software STAR CCM+ is used for the viscous flow computations. The Boundary Element Method (BEM) used in this paper is a self-developed perturbation potential based boundary element method, and the governing equation is

$$2\pi\phi(p) = \iint_{S_b} [\phi(q) \frac{\partial}{\partial n_q} \frac{1}{r(p;q)} - \frac{\partial\phi(q)}{\partial n_q} \frac{1}{r(p;q)}] dS + \iint_{S_w} \Delta\phi(q) \frac{\partial}{\partial n_q} \frac{1}{r(p;q)} dS \quad (1)$$

In equation (1), S_B denotes the body surface, and S_W denotes the wake surface. ϕ is the strength of perturbation potentials, or equivalent to the dipole strength, and $\partial\phi/\partial n$ is the source strength. $r(p;q)$ is the distance between the panel point q and the induced point p . The term $1/r$ is the potential induced by a unit strength source, and $\partial(1/r)/\partial n$ is the potential induced by a unit strength dipole. $\Delta\phi$ is the dipole strength in the wake from the Kutta condition, and the source strength in the wake is zero since the wake has no thickness. The discretized form of the equation (1) is

$$\sum_{j=1}^{N_p} a_{i,j} \phi_j = \sum_{j=1}^{N_p} b_{i,j} \frac{\partial\phi_j}{\partial n} - \sum_{m=1}^M \sum_{l=1}^{N_w} w_{i,m,l} \Delta\phi_{m,l} \quad i=1, N_p \quad (2)$$

In equation (2), ϕ_j and σ_j represent the discrete forms of ϕ and $\partial\phi/\partial n$; $a_{i,j}$ and $b_{i,j}$ represent the discrete forms of the integrations of $\partial(1/r)/\partial n$ and $1/r$ over a panel, respectively; w represents the discrete forms of the integration of $\partial(1/r)/\partial n$ over a wake panel. A wake alignment scheme is used in this boundary element method to correct the turbine blade wake geometry based on the induced velocities downstream, and a simple viscous correction is used for including the viscous effect. The turbine performances including the axial forces, torques, powers, pressure distributions and the circulation distributions can be obtained from the computations, and so are the pressure distributions and the circulation distributions.

The commercial software STAR CCM+ is used for the viscous flow computations. It solves the RANS equations by a finite volume method. The computational domain and boundary conditions are shown in Fig. 1, and the grid topology is shown in Fig. 2. Approximately 4 million polyhedral grids are normally used for the computations. A very dense mesh is adopted at tip of the blades in order to capture the phenomenon of the complex tip flow. Three turbulence models have been used for investigation, and they are “Realizable $k-\varepsilon$ two layer”, “standard $k-\varepsilon$ ” and “ $k-\omega$ SST”. If we use “Realizable $k-\varepsilon$ two layer” as reference, the differences are 1.31% and 0.55% for “standard $k-\varepsilon$ ” and “ $k-\omega$ SST” respectively. The STAR-CCM+ default turbulence model “realizable $k-\varepsilon$ two layer” is thus chosen for subsequent computations since these results are very close.

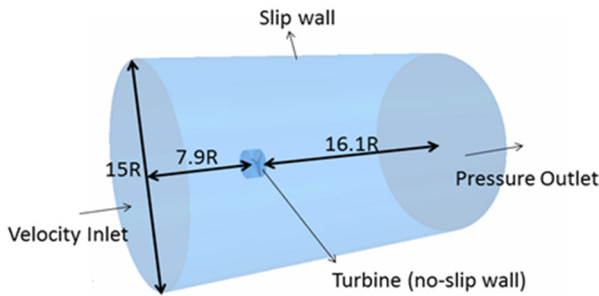


Fig. 1 Computational domain and boundary conditions for RANS computations

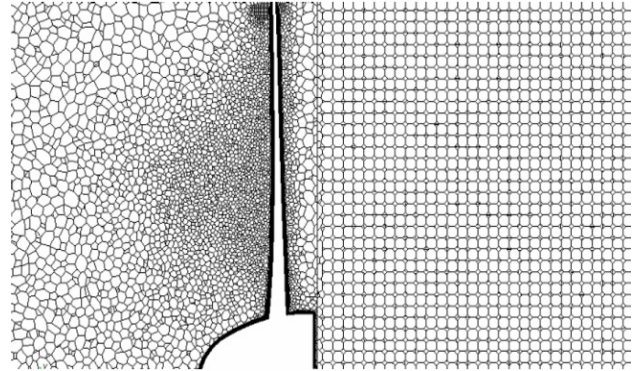


Fig. 2 The grid topology around current turbine

We then introduce several important coefficients related to the marine current turbine performance. These coefficients are the tip speed ratio (TSR), axial force coefficient (C_x), torque coefficient (C_Q) and power coefficient (C_{P_w}). They are defined as follows

$$TSR = \frac{2\pi nR}{V_\infty} \quad C_x = \frac{F_x}{\frac{1}{2}\rho AV_\infty^2}, \quad C_Q = \frac{Q}{\frac{1}{2}\rho AV_\infty^2 R}, \quad C_{P_w} = \frac{P_w}{\frac{1}{2}\rho AV_\infty^3} = TSR \times C_Q \quad (3)$$

In equation (3), R is the radius of turbine in meter, n is the rotational speed of turbine in rps, and V_∞ is the inflow velocity in m/s. F_x is the axial force working on turbine in N, Q is the torque working on turbine in N-m. P_w is the power of current turbine, and $P_w = 2\pi nQ$.

3. HYDRODYNAMIC DESIGN PROCEDURE AND RESULTS

The first design procedure is established based on the propeller design method. That is, the lifting line method is first used to obtain the optimum circulation distribution, or, the loading distribution. The Lagrange Multiplier Method is used to obtain the optimum circulation distribution. The Lagrange Multiplier Method can transfer a constrained problem to a non-constrained problem by introducing the Lagrange multiplier λ . For the current turbine blade design, the constrained optimization problem is to find a circulation distribution which provides the best power coefficient (C_{PW}), that is, the minimum axial force coefficient (C_X) with a given torque coefficient (C_Q). Therefore, the constraint is $C_Q = C_Q^*$, and C_Q^* is the objective torque coefficient. The design problem thus can be stated as

$$\begin{cases} \min & C_X \\ \text{subject to} & C_Q - C_Q^* = 0 \end{cases} \quad (4)$$

As described earlier, the torque coefficient and the axial force coefficient are functions of circulation distribution:

$$\begin{aligned} C_x &= C_x(\mathbf{\Gamma}) \\ C_Q &= C_Q(\mathbf{\Gamma}), \quad \mathbf{\Gamma} = [\Gamma_1, \Gamma_2, \dots, \Gamma_M]^T \end{aligned} \quad (5)$$

We thus can define the Lagrangian of this optimization problem as:

$$L(\mathbf{\Gamma}, \lambda) = C_X + \lambda(C_Q - C_Q^*) \quad (6)$$

To get the minimum value of C_X , we take the gradient of equation (6), and ∇L can be expressed as:

$$\begin{aligned} \nabla L &= \nabla C_X + \lambda \nabla C_Q = 0 \\ C_Q - C_Q^* &= 0 \end{aligned} \quad (7)$$

We can further derive to obtain:

$$\begin{aligned} \frac{\partial C_X}{\partial \Gamma_i} + \lambda \frac{\partial C_Q}{\partial \Gamma_i}, \quad \text{for } i = 1, \dots, M \\ C_Q - C_Q^* = 0 \end{aligned} \quad (8)$$

The optimum circulation distribution thus can be obtained by solving the equation, $G(\mathbf{X}) = 0$, and

$$G = \begin{bmatrix} \nabla L \\ C_Q - C_Q^* \end{bmatrix}, \quad \mathbf{X} = \begin{bmatrix} \mathbf{\Gamma} \\ \lambda \end{bmatrix} \quad (9)$$

Once the optimum circulation distribution is obtained, the blade geometry, namely, the pitch and the camber distributions can be obtained by the lifting surface vortex lattice method. The designs can then be verified by both BEM and RANS methods.

The second design procedure we used is based on the genetic algorithm method. This optimization method was inspired by Darwin's theory of evolution. The individual whose gene fit the environment better will have better potential for survival. After eliminating unsuitable individual for several generations, the remaining individuals indicate they might be the answer that we are looking for. Our objective is to design a new geometry of the current turbine that has a bigger C_Q and smaller C_X than the current turbine designed by the first procedure. In this procedure, the optimization method is the genetic algorithm, and the computations are carried out by the BEM. The reason is that it needs to compute the current turbine performance hundreds times for the genetic algorithm, and BEM method is much more efficient than the RANS method. We considered the pitch angle distributions as the gene in the individual. We designed a procedure that uses genetic algorithm to adjust the gene (pitch angle) to reach our objective (bigger torque and smaller axial force).

Table 1. The geometric parameters of the 20kW floating type current turbine

Foil Geometry	Number of blade	Radius (m)	Rotational speed (rps)	Inflow velocities (m/s)
NACA66/a = 0.8 meanline	3	5.0	0.5	1.5

Table 2. The force and power coefficients of the designed 20kW floating type current turbine

	C_x	$C_Q \cdot 10$	C_{PW}	Power (kW)
BEM	0.7074	0.7905	0.4139	13.687
RANS	0.7580	0.8634	0.4521	14.948

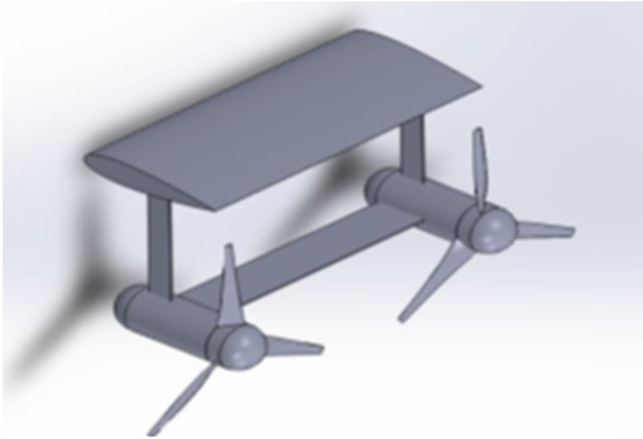


Fig. 3 The computer depiction of the 20kW Floating Kuroshio Turbine

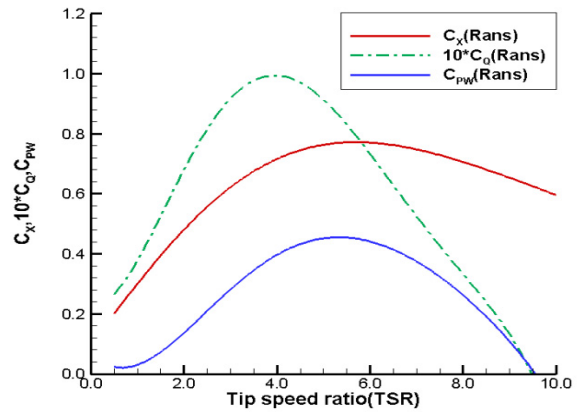


Fig. 4 The performance curves computed by RANS method

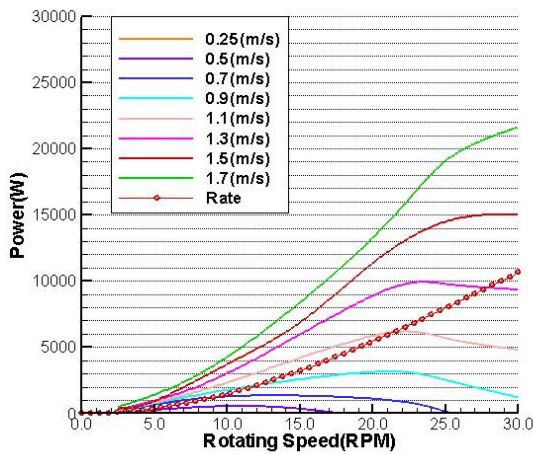


Fig. 5 The power curve computed by the RANS method. The line with circles is the rated power generated at different inflow speeds.

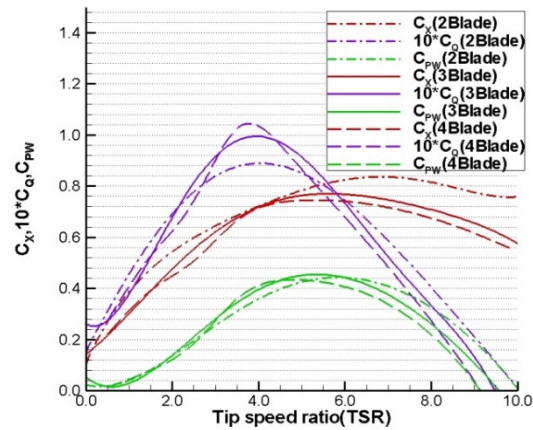


Fig. 6 the force and power coefficients of the designed geometry for different number of blades computed by the RANS method

We used the above procedures to design a 20kW Floating Kuroshio Turbine (FKT, shown as in Fig. 3). There are two sets of turbines for this 20kW current turbine, and each turbine should provide at least 10kW power. The geometric parameters are shown in Table 1, and the design torque is to have at least 4070 N-m ($C_Q = 0.07388$). For this design case, we are going to set the design goal to be the maximum power since we can have larger axial forces for the floating type current turbine. Therefore, the first procedure was used for an initial design, and the GA method was then used for the final designs. Table 2 shows the force and power coefficients of the designed geometry computed by the BEM and RANS methods. We can see that the torque coefficients are larger than the required one which means this design fulfills the design goal. The BEM is the computational method used in the GA method, and

the RANS method is the method to double check the design. Since the predicted power by RANS method is larger than the BEM, it means that both computational methods predict this design reaches the design goal. Fig. 4 shows the performance curves computed by RANS method, and Fig. 5 shows the power curve computed by the RANS method. In Fig. 5, the line with circles is the rated power of the electricity generator at different inflow speeds. Both Figs. 4 and 5 are important in the operation of the current turbine.

We have also designed blade geometries for different blade numbers, and Fig. 6 shows the force and power coefficients of the designed geometry for different number of blades computed by the RANS method. The BEM is the computational method used in two design procedures, and the RANS method is the method to double check the design. Since the predicted power by RANS method is larger than the BEM, it means that both computational methods predict this design reaches the design goal. Overall, the three blade geometry showed a promising and balanced performance.

4. STRUCTURE ANALYSIS AND POSSIBLE IMPROVEMENTS

After finishing the hydrodynamic design, we then applied the finite element method to analyze the structural strength of the blade, and the material we used is FRP. The FRP sandwich construction is shown in Fig. 7, and both the static pressure for water depth 50 meters and dynamic pressure are applied to the structure analysis. Fig. 8 shows the FEM grid, 115 grid points are distributed on the radial direction, and 50 grid points are distributed along the chord-wise direction. Totally we used 7100 elements for the core material, and 10300 elements on one side of FRP. The computational results show that the maximum blade deformation is at the blade tip, and the amount is 227 mm of the blade span 2.5 meters. The deformation rate is 9.1%. We have also obtained the Von Mises stress and Tsai-Wu value from computations. The Von Mises stress is 0.86 MPa under both static and dynamic pressure, and the strength of core material can satisfy the requirements of BV and DNVGL rules after including the safety factor. However, the maximum Tsai-Wu value indicates that FRP strength barely satisfy the rule requirements after considering the safety factor.

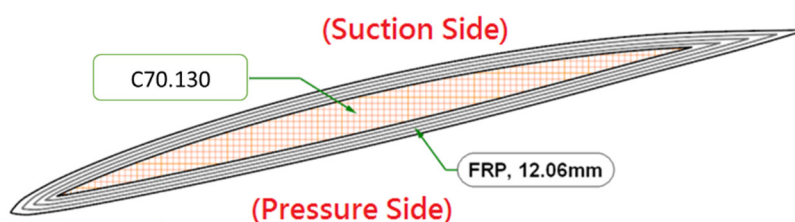


Fig. 7 The FRP sandwich construction of current turbine blade

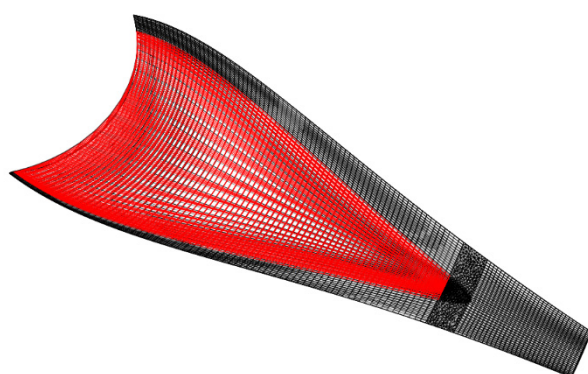


Fig. 8 Distribution of the FEM grid

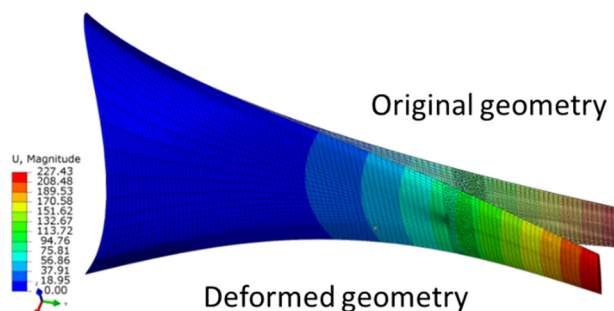


Fig. 9 Blade geometry deformation computed by FEM

There are many ways to improve the structural strength, and one of them is to simply increase the thickness of the FRP layer, make it stronger and more durable. The numerical results of increasing the thickness by 10%, 20% and 30% by RANS are investigated. The performances of FKT computed by RANS after increasing the blade thickness at the design point, TSR=5.19, are shown in Table 3. The thickness increased by 10% and 20% have the power decrease about 9%, and thickness increased by 30% has the largest difference, 18% decrease of the power. We thus focus on the thickness increased by 20% for further investigations.

Table 3. The performances of FKT computed by RANS after increasing the blade thickness at the design point, $TSR=5.19$

	C_T	Diff.	C_Q	Diff.
original	0.7580		0.8634	
thickness +10%	0.7523	-0.7%	0.7831	-9.3%
thickness +20%	0.7456	-1.6%	0.7861	-9.1%
thickness +30%	0.7206	-4.9%	0.7075	-18.1%

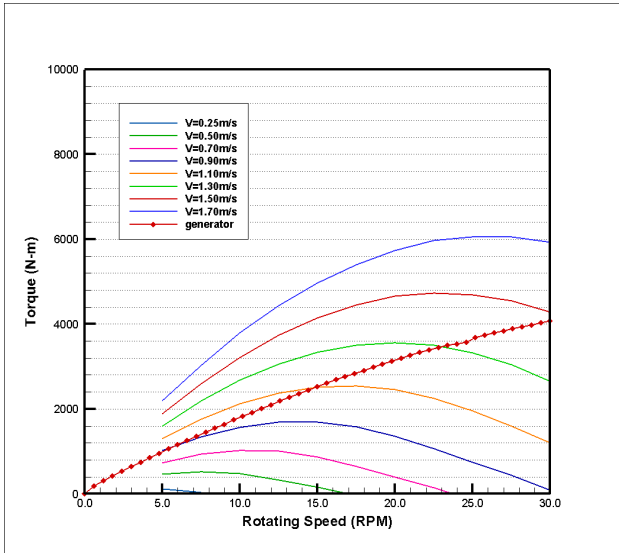


Fig. 10 The performance curve of torque of thickness increase by 20% (the new design) in different inlet velocities and rotating speeds

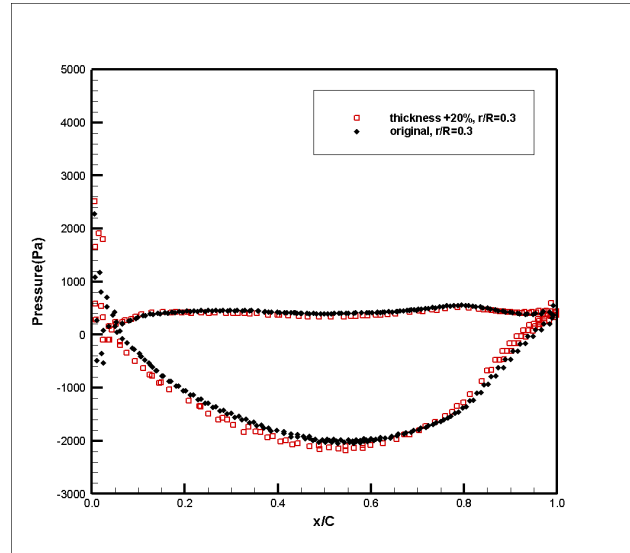


Fig. 11 The comparisons of pressure distribution of the original thickness and the new design at 0.3R

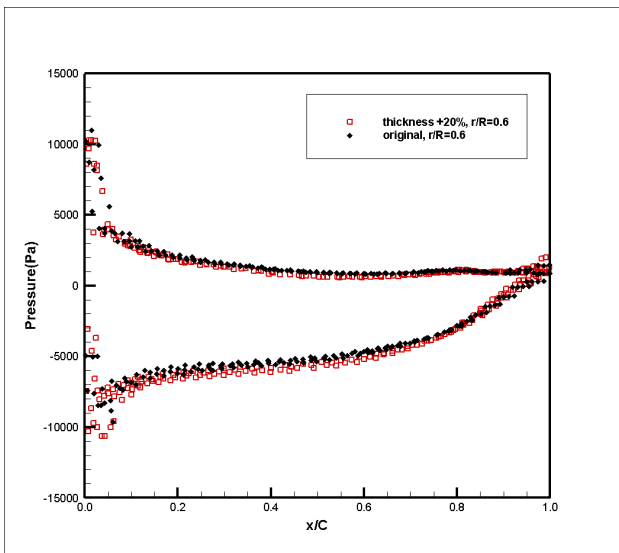


Fig. 12 The comparisons of pressure distribution of the original thickness and the new design at 0.6R

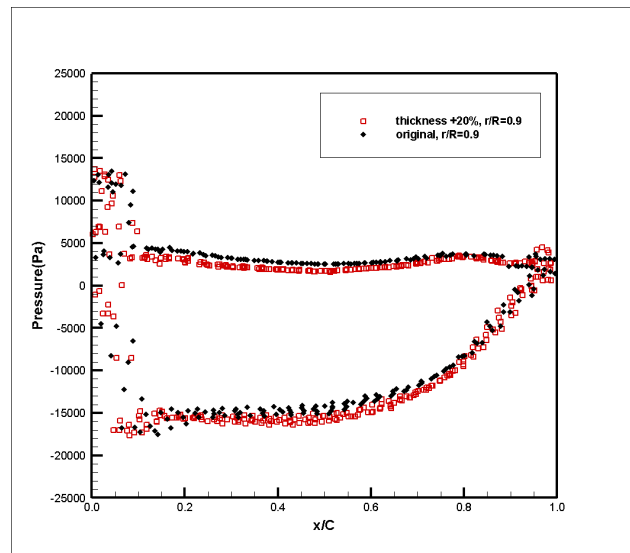


Fig. 13 The comparisons of pressure distribution of the original thickness and the new design at 0.9R

Fig. 10 shows the torque performance curve of thickness increased by 20% (the new design) in different inlet velocities and rotating speeds. Although the performance at design point decreases, the torque is still larger than the working torque of generator. That means the new design is capable of working with the generator which was chosen. Fig. 11 to Fig. 13 show the comparisons of pressure distributions computed by RANS of the original thickness and the new design at 0.3R, 0.6R and 0.9R, the black dot show the original design, and the red dots show the new design. One can see that although the performance of the new design is different from the original one, the pressure distributions are not very different. This means that the performance differences are mainly due to the viscous effects

from thicker blades. It also implies that the pressure loadings to the blade structure may not increase much due to thickness increase, and this should be confirmed by further FEM computations.

5. CONCLUSIONS

We have developed two different design procedures based on the Lagrange Multiplier method and Genetic Algorithm method respectively. The design of a 20kW Floating Kuroshio Turbine is demonstrated in the paper, and the design results show the geometry satisfies the hydrodynamic design goal. For the analysis, two Computational methods, RANS and BEM methods, are used to predict the performances of the current turbines, and both methods predict the similar trend. Finally, the structural strength of the turbine blade is computed by FEM, and the results show that the strength of core material can satisfy the requirements of BV and DNVGL rules after including the safety factor. However, the FRP strength barely satisfy the rule requirements after considering the safety factor. The blade thickness is thus increased by 10%, 20%, and 30%, and 20% is selected as the new design since the minimum decrease of the power. It is then found that the pressure distributions of the new design are not very different from the original design, and it may imply that the pressure loadings to the blade structure do not increase much by increasing the FRP layers.

ACKNOWLEDGEMENTS

This research project is funded by the Ministry of Science and Technology under National Energy Program, Phase II, Taiwan, R.O.C., MOST 104-3113-E-002-020-CC2. The authors would like to thank for the support.

REFERENCES

- [1] S. Goldstein, S., "On the vortex theory of screw propellers," *Proc. R. Soc. London Ser. A*, Vol. 123, pp. 440-465 (1929).
- [2] Lerbs, H.W. "Moderately loaded propellers with a finite number of blades and an arbitrary distribution of circulation," *SNAME Trans.*, Vol. 60, pp. 73-123 (1952).
- [3] Hsin, C.-Y., *Efficient Computational Methods for Multi-component Lifting Line Calculations*, M.S. Thesis, MIT, Cambridge, MA, USA (1986).
- [4] Kerwin, J.E., J.E., W.B. Coney, W.B., and C.-Y. Hsin, "Optimum circulation distributions for single and multi-component propulsors," *21st ATTC Conference*, Washington, DC, USA (1986).
- [5] Pien, P.C., "The calculation of marine propellers based on lifting surface theory," *J. Ship Res.*, Vol.5, pp. 1-14 (1961).
- [6] Kerwin, J.E., *The Solution of Propeller Lifting Surface Problems by Vortex Lattice Methods*, Report, Dept. of Ocean Eng., M.I.T., Cambridge, MA, USA (1961).
- [7] Greeley, D.S. and J.E. Kerwin, "Numerical methods for propeller design and analysis in steady flow," *SNAME Trans.*, Vol. 90, pp. 415-453 (1982).
- [8] Luo, Y.-S., *Investigation of the Current Turbine Performance by Computational Methods*, M.S. Thesis, National Taiwan Ocean University, Keelung, Taiwan (2013).
- [9] Wang, S.-Y., *Improvement of Marine Current Turbine Blade Design by Using the Genetic Algorithm*, M.S. Thesis, National Taiwan Ocean University, Keelung, Taiwan (2015).
- [10] Hsin, C.-Y., C. Ko, A.-C. Kuo and Y.-L. Tsai, "Applying different computational methods to the simulation of flow field around a horizontal axis marine current turbine," *12th Int. Conf. Fluid Control, Measurements and Visualization*, Nara, Japan (2013).
- [11] Hsin, C.-Y., Y.-S. Luo and C.-C. Lin "Applying the boundary element method to the analysis of flow around horizontal axis marine current turbines," *Proc. 8th Int. Workshop Ship Hydro.*, Seoul, South Korea (2013).
- [12] Bahaj, A.S., A.F. Molland, J.R. Chaplin, and W.M.J., "Power and thrust measurements of marine current turbines under various hydrodynamic flow conditions in a cavitation tunnel and a towing tank," *Renewable Energy*, Vol. 32, pp. 407-426 (2007).